Epitaxial Co-Au Superlattices

C. H. Lee, Hui He, F. Lamelas, W. Vavra, C. Uher, and Roy Clarke
Department of Physics, The University of Michigan, Ann Arbor, Michigan 48109
(Received 20 October 1988)

We demonstrate the growth of epitaxially ordered Co-Au superlattices by ultrahigh-vacuum deposition techniques. The superlattice structure consists of hcp Co(0001) and fcc Au(111) layers with the in-plane Co [11$\bar{2}$0] crystallographic axis parallel to GaAs [001]. X-ray scattering, high-resolution transmission-electron microscopy, and measurements of the magnetic anisotropy show that the Co-Au interfaces are abrupt even in the presence of a large lattice mismatch.

PACS numbers: 75.50.Rr, 68.55.−a, 81.15.Ef

There has been a great deal of interest in ultrathin ferromagnetic films in recent years stimulated in part by theoretical predictions of enhanced magnetic moments[1] and by new experimental developments in growth and characterization methods.[2] The magnetic anisotropy exhibited by some of these thin-film systems is particularly interesting from a fundamental standpoint as well as for applications to recording media. The anisotropy may arise in various ways, including magnetostriction, shape anisotropy, or from the reduced dimensionality of the structure at surfaces or interfaces.[3] While shape anisotropy generally favors an in-plane alignment of the magnetic easy axis, magnetocrystalline anisotropy may favor an easy axis perpendicular to the film plane, as is the case in Co(80)-Cr(20) alloy films grown in the *c*-axis orientation.[4] Surface or interface anisotropy[5] has been observed in ultrathin films; it is this anisotropy which is thought to be responsible for the perpendicular spin alignment in very thin single-layer films[6,7] and in superlattices prepared via evaporation,[8] rf sputtering,[9] and ion-beam sputtering[10] techniques. The quality of the interfaces bounding the magnetic layers in these systems is a key factor in establishing pronounced magnetic anisotropies.

Recent advances in ultrahigh-vacuum deposition techniques, particularly molecular-beam epitaxy (MBE), have opened up the exciting possibility of making high-quality magnetic heterostructures with reproducible characteristics. Rare-earth MBE superlattices, where good lattice matching exists, have been extensively studied.[11,12] There have been few studies, however, on the MBE growth of transition-metal ferromagnetic superlattices where lattice-matching conditions are generally harder to satisfy.[13]

In this Letter we demonstrate the use of MBE superlattice techniques to form superlattices with abrupt interfaces between ferromagnetic transition-metal (cobalt) layers and gold. The unprecedented control of structural quality that can be achieved by this growth technique permits epitaxial layer growth down to thicknesses of 5-Å cobalt. The superlattice layers are found to exhibit a high degree of epitaxial ordering *even in the presence of a large (≈ 14%) misfit* between hcp Co and fcc Au.

The superlattices in this study were grown on (110) GaAs substrates in a Vacuum Generators Model V80 MBE System. Our choice of Co and Au on GaAs as a superlattice system was motivated by earlier studies of the magnetic properties of annealed Co-Au sputtered multilayers[10] and by the work of Prinz on metastable bcc Co on GaAs.[14] Prior to film growth, the substrates were heated to 600 °C for 15 min in order to drive off impurities. A 500-Å epitaxial Ge(110) buffer layer was then grown at 600 °C on the annealed GaAs substrate in order to provide a smooth, clean surface for subsequent film growth. As indicated by reflection high-energy electron diffraction (RHEED), the epitaxial quality of the Ge layers improves markedly as the substrate temperature increases from 500 to 600 °C.

Following deposition of the buffer layer the substrates were cooled to 50 °C for superlattice growth. Au layers were grown at a rate of 0.080 ± 0.002 Å/sec out of a pyrolytic boren nitride Knudsen cell held at 1300 °C, and Co layers were grown out of an electron-beam hearth at approximately 0.3 Å/sec. Precise control of the Co flux was more difficult than for Au; therefore, the Co flux was integrated with a crystal monitor and this signal determined the open-close cycle time of the Co source. Background pressures prior to film growth were approximately 10^{-10} mbar, while pressures during superlattice growth were 10^{-9} mbar or better.

RHEED patterns were observed immediately after superlattice growth on the uppermost (Au) layer of the superlattice (Fig. 1) indicating that the films are oriented within the growth plane; the smoothness of the film surface is confirmed by the elongation of the RHEED streaks. The width of the streaks indicates that each film layer is broken up into an array of relatively small (20–30 Å) but epitaxially oriented domains. Given that the topmost Au layer of the superlattice is oriented within the growth plane, we may infer that all intervening Au and Co layers within the superlattice are also oriented. This is confirmed by detailed x-ray results discussed below.

Cross-sectional specimens (with the image plane per-

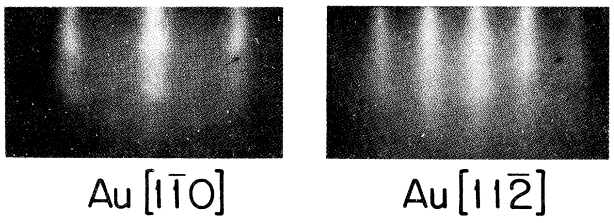

FIG. 1. RHEED patterns on Au top layer of Co(20 Å)-Au(16 Å) superlattice with the electron beam along the indicated Au crystal axes.

pendicular to the film plane) were prepared for conventional TEM and selected area diffraction measurements on a JEOL 2000 FX microscope, while atomic-resolution TEM images were obtained with a JEOL 4000 EX high-resolution electron microscope operated at 400 kV. The specimens were viewed along GaAs [1$\bar{1}$0] with the GaAs(110) surface parallel to the beam direction. TEM images (Fig. 2) show that the Co and Au layer thicknesses are uniform across the entire film. In addition, there is no evidence of interlayer mixing or disruption of the layers by the formation of Au or Co precipitates. High-resolution images of samples with a Ge buffer layer [Fig. 2, inset (a)] show that the Ge buffer layer is a single crystal grown epitaxially on the GaAs substrate. The high-resolution images also show Co and Au lattice fringes, indicating that uniform layering within the Co and Au layers extends over areas at least as large as the TEM specimen viewing area (about 300 Å).

A selected area diffraction pattern [Fig. 2, inset (b)], in which the TEM beam covers a region containing GaAs substrate, Ge buffer, and the Co-Au superlattice, shows sharp spots from the GaAs substrate and the epitaxial Ge buffer layer. Less intense and more elongated spots arise from the Co-Au superlattice and may be indexed in accord with Au growth in the (111) orientation with the Au [2$\bar{2}$0] axis parallel to the GaAs [001] axis, and with hcp Co growing in the (0001) orientation with the Co [11$\bar{2}$0] axis parallel to the Au [2$\bar{2}$0] axis.

While high-resolution TEM is a powerful technique for the investigation of interface quality, x-ray scattering is a more appropriate method to probe the stacking order of the layers.[15] X-ray diffraction measurements were carried out on a Huber four-circle diffractometer with a Rigaku 12-kW rotating Mo anode x-ray generator fitted with a graphite monochromator. A 00l low-angle scan performed in reflection geometry (with the scattering vector normal to the film plane) is shown in Fig. 3(a), along with the fit obtained from a superlattice model. In this one-dimensional model, we first construct a unit cell containing nominally 6 monolayers of Au and 11 monolayers of Co, repeated 20 times; then we incorporate interface interpenetration by varying the atomic scattering factor smoothly at Co-Au interfaces. We also include

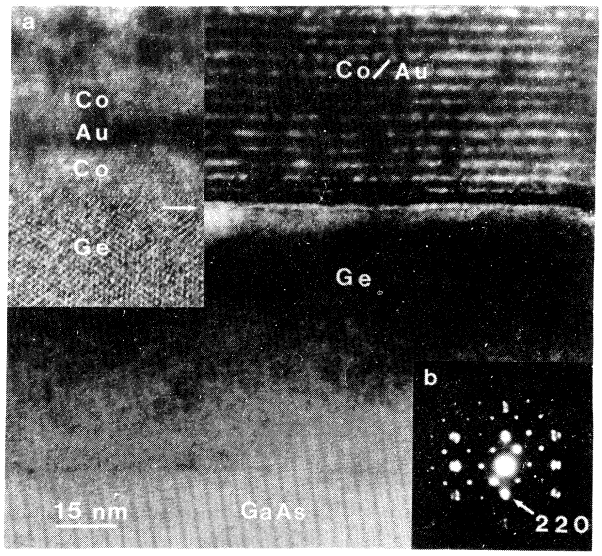

FIG. 2. Conventional TEM image of Co(20 Å)-Au(16 Å) superlattice on GaAs(110) with a 500-Å Ge buffer layer, taken with the electron beam along GaAs [1$\bar{1}$0]. Inset (a), high-resolution TEM image; inset (b), electron diffraction pattern.

source fluctuations by randomly varying the thickness of individual Co or Au layers. The fit shown in Fig. 3(a) was obtained by insertion of an interface width of 3 monolayers and random layer thickness fluctuations of ± 1.5 monolayers. Given the immiscibility of Au and Co in the bulk, we do not believe that diffusion occurs between Au and Co, but rather that local steps at the interface mimic the effect of diffusion in an x-ray scan [Fig. 3(a), inset].

In-plane scans [sometimes referred to as (hk0) scans], probe the epitaxial orientation of the films. These scans are performed in transmission through the film and substrate; thus it is necessary to mechanically thin the substrate to approximately 100 μm in order to allow sufficient penetration of the x-ray beam. Multiple scans are performed and a contour map of the in-plane scattering intensity is generated [Fig. 3(b), inset]. The in-plane contour maps show that the samples are highly oriented in the epitaxial plane and that both the fcc Au [2$\bar{2}$0] and hcp Co [11$\bar{2}$0] axes are parallel to the GaAs [001] axis, in accord with the TEM results. This orientation corresponds to a set of two parallel, close-packed lattices, differing only in the stacking of the atomic planes. hcp (rather than fcc) growth of the Co layers is indicated by the presence of the hcp Co(10$\bar{1}$0) peak at $2\theta = 18.8°$. (There is no corresponding fcc peak at this position.)

The separation of the in-plane Au(2$\bar{2}$0) and Co(11$\bar{2}$0) peaks [see Fig. 3(b), inset] indicates the presence of epitaxial mismatch in this system; the peaks are 3.6° apart in 2θ, rather than 4.4° as would be expected from the bulk lattice parameters of Co and Au. The average lat-

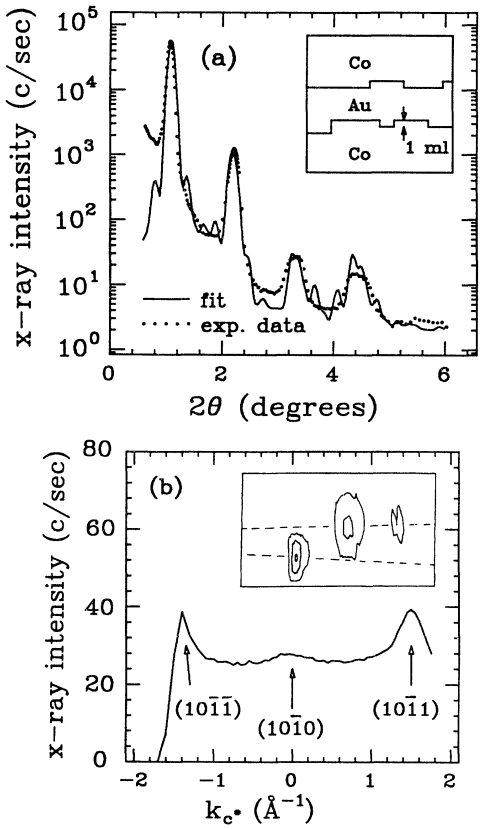

FIG. 3. (a) Low-angle x-ray data (points) of Co(20 Å)-Au(16 Å) superlattice and calculated intensity from the model described in the text. Inset: Schematic interface profile derived from the model. (b) X-ray diffraction profile along c^* (described in the text) showing hcp stacking of the Co layers. The rapid decrease in intensity at ~ -1.5 Å^{-1} is an experimental artifact. Inset: A portion of the in-plane diffraction intensity contour map; dashed lines pass through the origin. The peaks from left to right are GaAs(2$\bar{2}$2), Au(202), and Co($\bar{1}$2$\bar{1}$0).

tice spacing within the Au layers is found to be 1.25% compressed relative to the bulk value, whereas the Co spacing is expanded by the same amount. The width of the in-plane Au(2$\bar{2}$0) peak is 0.143 Å^{-1} corresponding to an in-plane correlation length of $\sim$22 Å. In view of the limited correlation length parallel to the interface, it is likely that the aforementioned peak shifts are caused by misfit dislocations rather than uniform elastic distortions. Interestingly, the presence of a relatively high mismatch at the interface does not seem to disrupt the layering or the long-range epitaxial orientation.

A second type of scan performed in transmission through the substrate, but with a scattering vector that may contain both in-plane and out-of-plane components, is the c^* scan. The c^* scan is sensitive to the stacking of crystal planes, and can be used to differentiate[15] between the *ABAB*... stacking of hcp (0001) planes and the

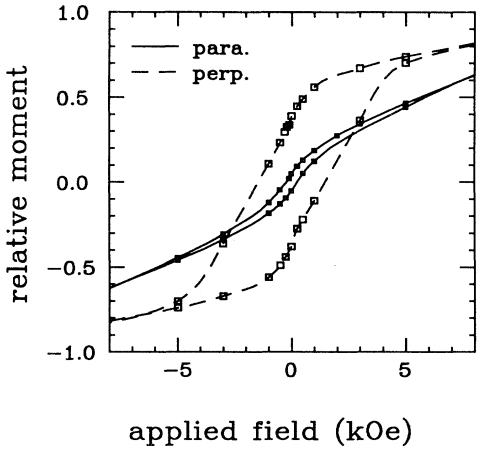

FIG. 4. Magnetic hysteresis loops measured at 5 K on a sample with 5-Å Co layers, with applied fields parallel (solid line) and perpendicular (dashed line) to the film plane.

ABCABC... stacking of fcc (111) planes. Figure 3(b) shows a c^* scan passing through the in-plane Co (10$\bar{1}$0) peak. The presence of the (10$\bar{1}\bar{1}$) and (10$\bar{1}$1) peaks at a spacing of $2\pi/2d_{(0002)}$ Å^{-1} above and below the (hk0) plane confirms the hcp stacking of the Co layers. A similar c^* scan passing through the Au(11$\bar{1}$) peak at a distance of $2\pi/3d_{(111)}$ Å^{-1} from the (hk0) plane confirms the fcc stacking of the Au layers.

In order to demonstrate the anisotropy crossover in our samples, we performed magnetic measurements on five samples with Co layer thicknesses in the range 5–40 Å and constant Au spacer layers of $\sim$16 Å in a Quantum Design MPMS SQUID (superconducting quantum interference device) magnetometer. Hysteresis loops were measured with applied fields of up to 15 kOe both parallel and perpendicular to the substrate plane at sample temperatures ranging from 5 to 300 K. We have observed the shift of the magnetic easy axis out of the film plane as Co layer thickness is decreased (see Fig. 4); the crossover appears to occur at $\approx$20-Å Co. This shift in the easy axis has been reported previously in the sputtered Co-Au multilayers of den Broeder *et al.*[10] which required annealing at 250°C in order to improve the Co-Au interface sharpness. Note that in our samples the perpendicular anisotropy is evident in the as-grown films, with no annealing necessary. This result indicates that the Co-Au interfaces are intrinsically sharper in the MBE grown films, which is not surprising, given the different growth conditions occurring in MBE and the sputtering process. We have also observed a strong and unusual temperature dependence of the coercivity in perpendicular field: In samples with a perpendicular easy axis, the coercivity increases significantly (from 150 to 1500 kOe) at low temperatures. The magnetic behavior will be described in detail elsewhere.

Given the structural data presented above, we can un-

derstand the growth of Co-Au superlattices as follows. Starting with a smooth Ge(110) surface, our RHEED observations show that the first Co layer deposited grows in the bcc (110) orientation, in accord with the bcc Co growth on GaAs reported by Prinz.[14] However, when the first Au layer is deposited, the orientation and symmetry of the growing film is shifted to Au (111). This shift is driven by the lower surface energy of the (close-packed) Au(111) surface. Once the first Au layer has relaxed to (111) growth, succeeding Co layers will no longer impinge upon a surface favoring bcc growth. Cobalt deposited on the Au(111) surface apparently fills the close-packed sites present and proceeds to stack in the hcp *ABAB* . . . sequence.

The 14.5% lattice mismatch between the Au and Co close-packed planes is taken up by misfit dislocations and the consequent formation of small but epitaxially oriented in-plane domains. A rough prediction of the size of these domains, determined by the vernier distance, is the average near-neighbor distance divided by the lattice mismatch, in this case 2.7 Å/0.145 = 18.6 Å, which agrees will with the 22 Å estimated from the width of the in-plane peaks, as discussed above. It is this small domain size which leads to broadening of the Au surface RHEED streaks shown in Fig. 1.

We conclude that, in spite of the large mismatch between Au and Co, the interfaces are sharp aside from the presence of local steps at the monolayer level. The superlattices exhibit desirable magnetic anisotropies in the as-grown condition without the need for subsequent annealing. These systems are also interesting candidates for a series of detailed structural, magnetic, and transport measurements.

We are grateful to G. Vezzoli, MTL Watertown, MA, for his initial support of this project. The work was also supported in part by NSF Materials Research Group Grant No. DMR 8602675. We acknowledge useful discussions with A. J. Freemen and thank H. M. Naik for her help during the course of this work. TEM studies were performed with the assistance of K. Chang, University of Michigan EMAL. One of us (F.L.) was supported by a U.S. Army Research Office Grant No. DAAL-03-86-G-0053.

[1]C. L. Fu, A. J. Freeman, and T. Oguchi, Phys. Rev. Lett. **54**, 2700 (1985); J. G. Gay and R. Richter, Phys. Rev. Lett. **56**, 2728 (1986).

[2]B. Heinrich, A. S. Arrott, J. F. Cochran, C. Liu, and K. Myrtle, J. Vac. Sci. Technol. A **4**, 1376 (1986); C. Rau, C. Liu, A. Schmalzbauer, and G. Xing, Phys. Rev. Lett. **57**, 2311 (1986).

[3]R. M. Bozorth, *Ferromagnetism* (Van Nostrand, Princeton, 1951).

[4]S. Iwasaki and K. Ouchi, IEEE Trans. Magn. **14**, 849 (1978).

[5]U. Gradmann, J. Magn. Magn. Mater. **54–57**, 733 (1986).

[6]C. Chappert, K. LeDang, P. Beauvillain, H. Hurdequint, and D. Renard, Phys. Rev. B **34**, 3192 (1986).

[7]C. Liu, E. R. Moog, and S. D. Bader, Phys. Rev. Lett. **60**, 2422 (1988).

[8]H. J. G. Draaisma and W. J. M. deJonge, J. Magn. Magn. Mater. **66**, 351 (1987).

[9]P. F. Carcia, A. D. Meinhaldt, and A. Suna, Appl. Phys. Lett. **47**, 178 (1985).

[10]F. J. A. den Broeder, D. Kuiper, A. P. van de Mosselaer, and W. Hoving, Phys. Rev. Lett. **60**, 2769 (1988).

[11]J. Kwo, E. M. Gyorgy, D. B. McWhan, E. M. Hong, F. J. DiSalvo, C. Vettier, and J. E. Bower, Phys. Rev. Lett. **55**, 1402 (1985).

[12]M. B. Salamon, S. Sinha, J. J. Rhyne, J. E. Cunningham, E. Ross, J. Borchers, and C. P. Flynn, Phys. Rev. Lett. **56**, 259 (1986).

[13]H. K. Wong, H. Q. Yang, J. E. Hilliard, and J. B. Ketterson, J. Appl. Phys. **57**, 3660 (1985).

[14]G. A. Prinz, Phys. Rev. Lett. **54**, 1051 (1985).

[15]Roy Clarke, F. Lamelas, C. Uher, C. P. Flynn, and J. E. Cunningham, Phys. Rev. B **34**, 2022 (1986).

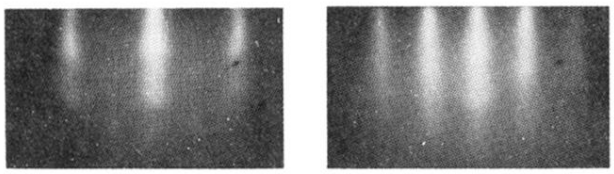

FIG. 1. RHEED patterns on Au top layer of Co(20 Å)-Au(16 Å) superlattice with the electron beam along the indicated Au crystal axes.

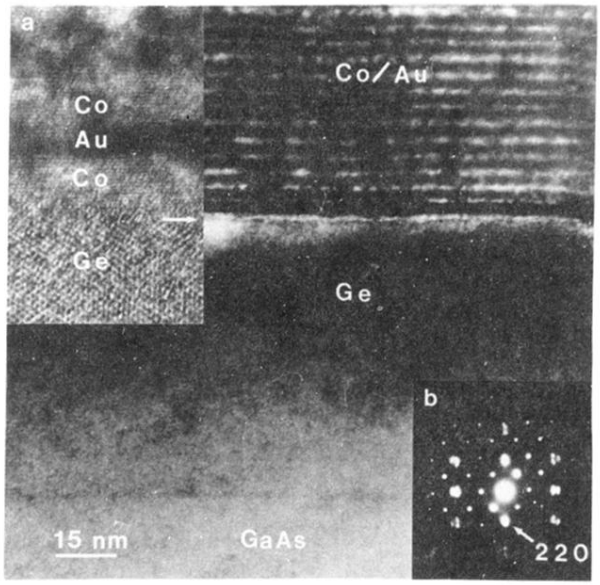

FIG. 2. Conventional TEM image of Co(20 Å)-Au(16 Å) superlattice on GaAs(110) with a 500-Å Ge buffer layer, taken with the electron beam along GaAs [1$\bar{1}$0]. Inset (a), high-resolution TEM image; inset (b), electron diffraction pattern.